Sensors and Materials, Vol. 32, No. 8 (2020) 2569–2576
MYU Tokyo

S & M 2283

Carbon Dioxide Sensing Characteristics of AlGaN/GaN High Electron Mobility Transistor with ZnO Nanorods

Kwang Hyeon Baik[1] and Soohwan Jang[2*]

[1]Department of Materials Science and Engineering, Hongik University,
2639 Sejong-ro, Jochiwon, Sejong 30016, Republic of Korea
[2]Department of Chemical Engineering, Dankook University,
152 Jukjeon-ro, Suji-gu, Yongin-si, Gyeonggi-do 16890, Republic of Korea

(Received April 7, 2020; accepted June 2, 2020)

Keywords: carbon dioxide, gas sensor, AlGaN/GaN, HEMT, ZnO

A CO_2 sensor based on an AlGaN/GaN high electron mobility transistor (HEMT) was developed using ZnO nanorods as the sensing material. The sensor showed a reliable response to a wide range of CO_2 concentrations from 500 to 100000 ppm at 300 °C. The CO_2 response of the device was tested from 25 to 400 °C, and the sensor started to exhibit responsivity to 30000 ppm CO_2 gas at 150 °C. The responsivity increased with the ambient temperature until the temperature reached 300 °C, and it decreased from 350 to 400 °C. The maximum responsivity of the sensor with ZnO nanorods was 4.31% for 10% CO_2 exposure at 300 °C. In addition, the effect of humidity on the CO_2 sensing characteristics was investigated. AlGaN/GaN-heterostructure-based CO_2 sensors functionalized with ZnO nanorods have high potential for applications in the chemical, medical, energy, and food industries.

1. Introduction

There has been much interest in CO_2 sensors for monitoring global warming, indoor air quality, process control in fermentation, and medical use.[1,2] The concentration of atmospheric CO_2 was 280 ppm before the industrial revolution, which increased to 400 ppm with the increase in fossil fuel usage.[3] CO_2 is colorless and odorless, and its molecular mass is 44.01 g/mol, which is heavier than air (18.02 g/mol). Hence, it easily accumulates on the ground of an enclosed space. A CO_2 concentration of more than 7% can cause acute symptoms in exposed people including unconsciousness, even in environments with high concentrations of oxygen. For example, a worker in an isolated septic tank with a high concentration of CO_2 can become unconscious and die in severe cases. CO_2 is used for reactants, intermediates, and products in the chemical, medical, energy, and food industries. It is necessary to detect promptly the specific concentration of CO_2 for the safety of workplaces and the health of workers, as well as to monitor indoor air quality in daily life.

The most conventional approach to detecting CO_2 is based on nondispersive infrared absorption sensors, which consist of an infrared source, a light tube, an interface filter,

*Corresponding author: e-mail: jangmountain@dankook.ac.kr
https://doi.org/10.18494/SAM.2020.2900

ISSN 0914-4935

and an infrared detector.[4,5] They have good sensitivity and selectivity for CO_2 sensing, but they require high power consumption, a large physical space, and a complex structure. Semiconductor-based gas sensors have many merits, such as low power consumption, compact size, sensitivity, and reliability.[5] Among the many semiconductor materials, GaN-based material systems are highly suitable for gas sensing. GaN-based gas sensors exhibit high signal-to-noise ratios, and they have reliable and stable operation at high temperatures owing to their excellent material properties, such as a wide energy bandgap of 3.4 eV, chemical and mechanical robustness, excellent carrier transport, and radiation hardness.[6–24] One of the biggest advantages of GaN-based semiconductors is the availability of the AlGaN/GaN heterostructure, in which a two-dimensional electron gas (2DEG) channel with a mobility of more than 1500 $cm^2/V{\cdot}s$ forms at the interface between AlGaN and GaN due to spontaneous polarization and piezoelectric effects.[6–9,18–24] The electron conductivity of the 2DEG is sensitive to changes in charge on the top AlGaN surface. In the sensor structure of an AlGaN/GaN high electron mobility transistor (HEMT), the gate region is functionalized with a specific catalytic material to induce the decomposition reaction of the target gas. This results in a change in surface charge on the AlGaN surface. Monitoring the drain current passing through the 2DEG in the HEMT enables the output sensing signal for the decomposition reaction of the target gas to be obtained.

ZnO is a direct-bandgap semiconducting material with a wide bandgap energy of 3.37 eV and a large exciton binding energy of 60 meV.[25–27] ZnO nanostructures are grown by a simple hydrothermal method, which is a low-cost, nontoxic, low-temperature, and scalable process. During hydrothermal growth, the growth rate of the *c*-plane is higher than that of the *m*-plane in the wurtzite crystal structure because of the higher surface energy of the *c*-plane; ZnO nanowires or bundles of nanorods along the *c*-axis are generally formed during the hydrothermal synthesis process.[27–30] These ZnO nanorods with high surface-to-volume ratio can be employed in AlGaN/GaN HEMT gas sensors in the gate region to achieve high sensitivity to the target gas.

In this research, an AlGaN/GaN HEMT-based CO_2 sensor using ZnO nanorods as a sensing material was fabricated, and its CO_2 sensing characteristics were investigated. The effects of temperature, CO_2 concentration, and humidity on the CO_2 responsivity were studied.

2. Materials and Methods

The AlGaN/GaN heterostructure was grown by metal organic chemical vapor deposition on a *c*-plane Al_2O_3 substrate.[6–9] The epitaxial layer consisted of 2.5 μm GaN and 30 nm $Al_{0.3}GaN$. The sheet resistance, sheet carrier concentration, and carrier mobility of the AlGaN/GaN heterostructure were 320 ohm/square, 9×10^{12} cm^{-2}, and 1800 $cm^2/V{\cdot}s$, respectively. Figure 1 shows a top-view scanning electron microscopy (SEM) image of the HEMT with ZnO nanorods on the gate region and a schematic cross-sectional diagram of the HEMT structure along the cutline of A–A' in (a). The fabrication of the device started with 75 nm mesa isolation achieved by inductively coupled plasma etching with Ar/Cl_2 gas. A 20 nm Ti/80 nm Al/40 nm Ni/80 nm Au metal stack was deposited by electron beam

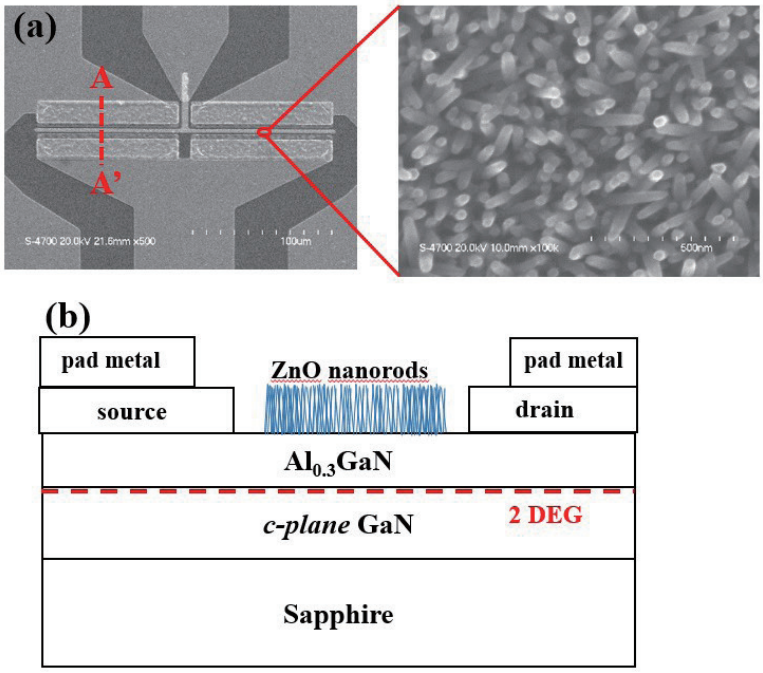

Fig. 1. (Color online) (a) Top-view SEM image of the HEMT with ZnO nanorods and enlarged image of the ZnO nanorods. (b) Schematic cross-sectional diagram of the HEMT structure along the cutline of A–A' in (a).

evaporation, and the stack was annealed at 950 °C for 1 min under a N_2 atmosphere by rapid thermal annealing for ohmic contact formation. A 20 nm Ti/120 nm Au pad metal was formed by electron beam evaporation for electrical signal probing. ZnO nanorods were selectively grown on the gate area by conventional photolithography, a simple hydrothermal ZnO nanorod growth method,[27–30] and a lift-off process. A 25 mM solution of zinc nitrate hexahydrate was dissolved in deionized water, and a 25 mM methenamine solution was prepared. These two solutions were mixed together equivolumetrically in a Teflon-lined autoclave to prepare a growth solution. The fabricated AlGaN/GaN HEMT substrate was suspended upside down in the growth solution and was placed in a 90 °C oven for 90 min. After the growth, the sample was removed, washed with deionized water vigorously, and blow-dried with nitrogen. This growth cycle was repeated five times to obtain dense ZnO nanorods with a high aspect ratio. The length and diameter of the ZnO nanorods were approximately 1 μm and 50 nm, respectively.

The drain current–voltage characteristics and current response of the HEMT sensor with ZnO nanorods were measured using an Agilent 4156C semiconductor parameter analyzer with the device in a gas test chamber under ambient conditions of various concentrations of CO_2 in air. The temperature and humidity of the test ambient conditions were controlled respectively by the heater chuck on which the sample was placed and the humidity controller connected to the gas test chamber.

3. Results and Discussion

Figure 2 shows the drain *I–V* characteristics of the AlGaN/GaN HEMT with ZnO nanorods under air and a 10% CO_2 atmosphere at 300 °C. When the device was exposed to CO_2 gas, the drain current increased. In the AlGaN/GaN heterostructure, a 2DEG channel layer exists underneath the AlGaN owing to polarization and piezoelectric effects, as shown in Fig. 1(b).[6–9,18,19] The conductivity of the 2DEG channel was affected sensitively by the change in charge on the AlGaN surface. If a reaction inducing the change in surface charge on the AlGaN surface by a target gas occurs, the conductivity of the 2DEG changes, resulting in a change in the drain current of the AlGaN/GaN HEMT. In the case of the CO_2 atmosphere, the possible sensing mechanism of the AlGaN/GaN HEMT with ZnO nanorods is described as follows. ZnO is known to adsorb oxygen ions on the surface.[1,2,5] The exposed CO_2 gas molecules react with the adsorbed O^- and release electrons with a negative charge. These electrons make the oxide more negative and induce an additional positive charge on the AlGaN surface, which enhances the 2DEG channel by accumulating more electrons and increasing the drain current of the device.

$$CO_2\,(g) + O^-(ad) \leftrightarrow CO\,(g) + O_2\,(g) + e^- \tag{1}$$

It is notable that the increase in drain current upon CO_2 exposure is opposite to the case of reducing NH_3 gas in an AlGaN/GaN HEMT with ZnO nanorods.[20,21]

The responses of the AlGaN/GaN HEMT functionalized by ZnO nanorods to sequential 10 s exposures of 100% N_2 and 300–100000 ppm CO_2 in dry air at 150 and 300 °C are shown in Fig. 3. The drain bias voltage was fixed at 1 V. The device was tested under the same conditions at 25 to 400 °C in 50 °C increments, but no response to CO_2 was observed at 25, 50, and 100 °C. At 150 °C, the HEMT with ZnO nanorods started to respond to 30000 ppm CO_2, but the drain current signal was unclear. In contrast, distinctive changes in current for exposures to various

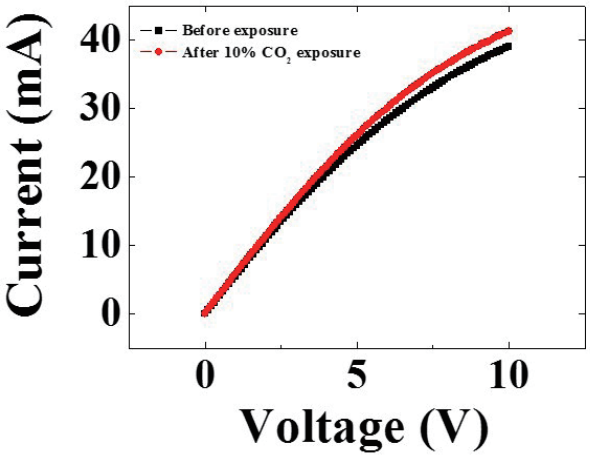

Fig. 2. (Color online) Drain current response of the HEMT sensor to air and 10% CO_2 exposure at 300 °C.

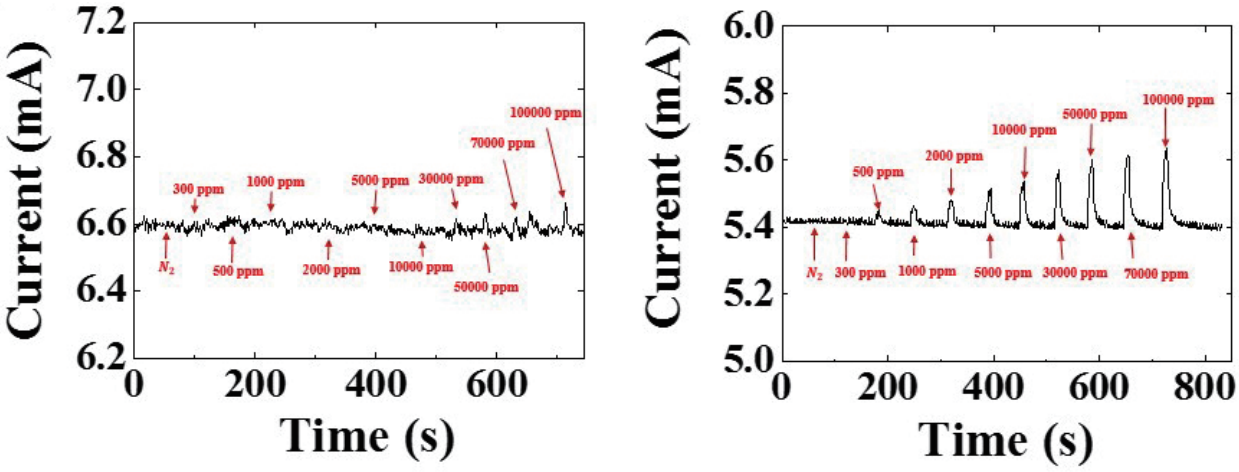

Fig. 3. (Color online) Time-dependent responses of the HEMT to 100% N_2 and 300–100000 ppm CO_2 at 150 and 300 °C. The drain bias was 1 V and the gas exposure time was 10 s.

concentrations of CO_2 were observed at 300 °C. The drain current returned to the original level after switching back to air. The minimum measurable concentration of CO_2 was 500 ppm. The AlGaN/GaN HEMT with ZnO nanorods showed reliable repeatability for cyclic exposures with various concentrations of CO_2 at 300 °C.

Figure 4 shows the responsivity of the HEMT sensor to 300–100000 ppm (10%) concentrations of CO_2 at 150, 200, 250, 300, 350, and 400 °C. The responsivity is defined as $(I_{CO_2} - I_{air}) / I_{CO_2} \times 100$ (%), where I_{CO_2} and I_{air} are the drain currents of the HEMT at 1 V under CO_2 and ambient air, respectively. As the CO_2 concentration increases, the responsivity increases and saturates at high CO_2 concentrations. The HEMT responsivity for 10% CO_2 at 300 °C was 4.31%. The responsivity increased with the ambient temperature until reaching 300 °C, and it decreased at 350 and 400 °C. The oxygen ions adsorbed on the ZnO surface exist in the form of O_2^-, O^-, and O^{2-}. The O_2^-, O^-, and O^{2-} ions are stable below 100 °C, between 100 and 300 °C, and above 300 °C, respectively.[1,31] The rate of the forward reaction of Reaction (1) may increase with the concentration of adsorbed oxygen ions, O^-, up to 300 °C; hence, the device shows maximum responsivity at 300 °C. This temperature dependence of the responsivity can also be found in the case of ZnO thin-film CO_2 sensors.[1]

The responsivity at 300 °C was modeled using the dissociative Langmuir isotherm given below, as shown in Fig. 5,[6,32]

$$R = \frac{\alpha \left(K_{eq} \cdot C \right)^{\frac{1}{2}}}{1 + \left(K_{eq} \cdot C \right)^{\frac{1}{2}}}, \tag{2}$$

where R is the responsivity, α is the proportionality constant, K_{eq} is the equilibrium constant of the adsorption, and C is the concentration of CO_2. The plot shows good agreement with the

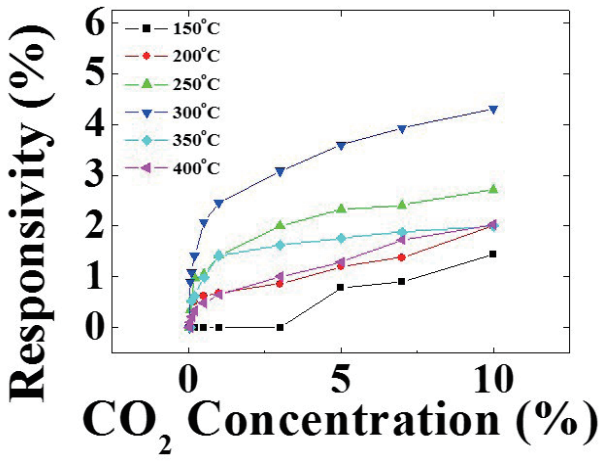

Fig. 4. (Color online) Responsivity of the HEMT sensor to different concentrations of CO_2 at 150, 200, 250, 300, 350, and 400 °C.

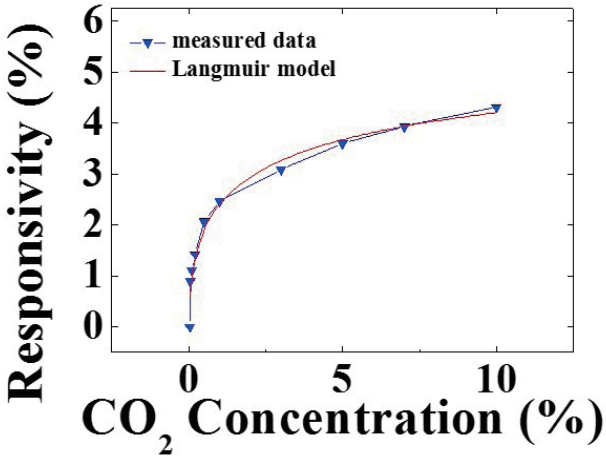

Fig. 5. (Color online) Responsivity of the HEMT to different concentrations of CO_2 at 300 °C and its Langmuir isotherm fitting model.

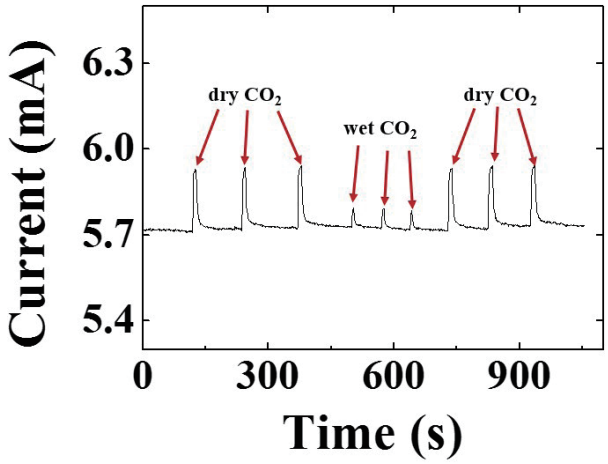

Fig. 6. (Color online) Change in drain current of the HEMT at 300 °C for cyclic exposures of dry, wet, and dry 10% CO_2.

measured and calculated data. The equilibrium constant of the AlGaN/GaN HEMT with ZnO nanorods at 300 °C was 0.346.

The effect of humidity on CO_2 sensing was investigated. Figure 6 shows the change in drain current of the HEMT with ZnO nanorods at 300 °C for cyclic exposures of dry, wet, and dry 10% CO_2. The bias voltage was 1 V, and each 10 s of CO_2 exposure was repeated three times. The relative humidity was 77% for a wet CO_2 environment at 300 °C. The change in drain current decreased by 64% under a humid ambient condition compared with the case of dry CO_2 exposure, even at a high temperature of 300 °C. Under wet CO_2 conditions, H_2O molecules were adsorbed on the surface of ZnO nanorods and prevented CO_2 molecules from reacting with oxygen ions on the active sites of the nanorods, reducing the change in drain current.[25]

This deteriorating effect of humidity can be overcome by employing polyimide-based moisture barrier encapsulation with a high glass transition temperature, which enables CO_2 molecules to penetrate but blocks H_2O.[6–9,25]

5. Conclusions

An AlGaN/GaN HEMT with ZnO nanorods on the gate region was shown to be capable of CO_2 detection from 150 °C. The device demonstrated reliable sensing characteristics for the CO_2 concentration range from 500 to 100000 ppm at 300 °C. The maximum responsivity of the sensor for 10% CO_2 exposure was 4.31%. The CO_2-sensing capability of the HEMT increased with ambient temperature until it reached 300 °C; then, it decreased at 350 and 400 °C. When wet CO_2 was introduced to the HEMT sensor, the responsivity dropped by 64% at 300 °C because the active sites of the ZnO nanorods were blocked by H_2O molecules.

Acknowledgments

This research was supported by the Basic Science Research Program through the National Research Foundation of Korea (NRF) funded by the Ministry of Education (2018R1D1A1A09083988, 2020R1I1A3A0403783711), and the Nano·Material Technology Development Program through the NRF funded by the Ministry of Science, ICT and Future Planning (2015M3A7B7045185).

References

1 P. K. Kannan, R. Saraswathi, and J. B. Rayappan: Ceram. Int. **40** (2014) 13115. https://doi.org/10.1016/j.ceramint.2014.05.011
2 O. Lupan, L. Chow, S. Shishiyanu, E. Monaico, T. Shishiyanu, V. Sontea, B. R. Cuenya, A. Naitabdi, S. Park, and A. Schulte: Mater. Res. **44** (2009) 63. https://doi.org/10.1016/j.materresbull.2008.04.006
3 R. Monastersky: Nature **497** (2013) 7447. https://doi.org/10.1038/497013a
4 T. A. Vincent and J. W. Gardner: Sens. Actuators, B **236** (2016) 954. https://doi.org/10.1016/j.snb.2016.04.016
5 T. Anderson, F. Ren, S. Pearton, B. S. Kang, H. Wang, C. Chang, and J. Lin: Sensors **9** (2009) 4669. https://doi.org/10.3390/s90604669
6 K. H. Baik, S. Jung, F. Ren, S. J. Pearton, and S. Jang: ECS J. Solid State Sci. Technol. **7** (2018) Q3009. https://doi.org/10.3390/s90604669
7 S. Jung, K. H. Baik, F. Ren, S. J. Pearton, and S. Jang: IEEE Sens. J. **17** (2017) 5817. https://doi.org/10.1109/JSEN.2017.2733343
8 S. Jung, K. H. Baik, and S. Jang: ECS Trans. **77** (2017) 33. https://doi.org/10.1149/07706.0033ecst
9 S. Jung, K. H. Baik, F. Ren, S. J. Pearton, and S. Jang: IEEE Electron Device Lett. **38** (2017) 657. https://doi.org/10.1109/LED.2017.2681114
10 S. Jang, S. Jung, and K. H. Baik: Thin Solid Films **660** (2018) 646. https://doi.org/10.1016/j.tsf.2018.04.027
11 S. Jang, P. Son, J. Kim, S. Lee, and K. H. Baik: Sens. Actuators, B **222** (2016) 43. https://doi.org/10.1016/j.snb.2015.08.056
12 H. Kim, K. H. Baik, F. Ren, S. J. Pearton, and S. Jang: ECS Trans. **61** (2014) 353. https://doi.org/10.1149/06104.0353ecst
13 K. H. Baik, H. Kim, S. Lee, E. Lim, S. J. Pearton, F. Ren, and S. Jang: Appl. Phys. Lett. **104** (2014) 072103. https://doi.org/10.1063/1.4866010
14 Y. L. Wang, F. Ren, W. Lim, S. J. Pearton, K. H. Baik, S. Hwang, Y. G. Seo, and S. Jang: Curr. Appl. Phys. **10** (2010) 1029. https://doi.org/10.1016/j.cap.2009.12.034
15 K. H. Baik, J. Kim, and S. Jang: Sens. Actuators, B **238** (2017) 462. https://doi.org/10.1016/j.snb.2016.07.091

16 S. Jang, J. Kim, and K. H. Baik: J. Electrochem. Soc. **163** (2016) B456. https://doi.org/10.1149/2.1161608jes
17 K. H. Baik, J. Kim, and S. Jang: ECS Trans. **72** (2016) 23. https://doi.org/10.1149/07205.0023ecst
18 H. Kim and S. Jang: Curr. Appl. Phys. **13** (2013) 1746. https://doi.org/10.1016/j.cap.2013.07.008
19 H. Kim, W. Lim, J. Lee, S. J. Pearton, F. Ren, and S. Jang: Sens. Actuators, B **164** (2012) 64. https://doi.org/10.1016/j.snb.2012.01.067
20 S. Jung, K. H. Baik, F. Ren, S. J. Pearton, and S. Jang: ECS J. Solid State Sci. Technol. **7** (2018) Q3020. https://doi.org/10.1149/2.0041807jss
21 S. Jung, K. H. Baik, F. Ren, S. J. Pearton, and S. Jang: J. Vac. Sci. Technol. B. **35** (2017) 042201. https://doi.org/10.1116/1.4989370
22 S. Jung, K. H. Baik, F. Ren, S. J. Pearton, and S. Jang: J. Electrochem. Soc. **164** (2017) B417. https://doi.org/10.1149/2.0781709jes
23 S. Jung, K. H. Baik, and S. Jang: ECS Trans. **77** (2017) 121. https://doi.org/10.1149/07706.0121ecst
24 S. Jung, K. H. Baik, and S. Jang: ECS Trans. **75** (2017) 9. https://doi.org/10.1149/07540.0009ecst
25 S. Jang, S. Jung, and K. H. Baik: Sensors **20** (2020) 835. https://doi.org/10.3390/s20030835
26 S. Jang, S. Jung, and K. H. Baik: ECS J. Solid State Sci. Technol. **8** (2019) Q85. https://doi.org/10.1149/2.0131904jss
27 J. Kim, K. H. Baik, and S. Jang: Curr. Appl. Phys. **16** (2016) 221. https://doi.org/10.1016/j.cap.2015.11.014
28 K. H. Baik, H. Kim, J. Kim, S. Jung, and S. Jang: Appl. Phys. Lett. **103** (2013) 091107. https://doi.org/10.1063/1.4819847
29 L. E. Greene, M. Law, J. Goldberger, F. Kim, J. C. Johnson, Y. Zhang, R. J. Saykally, and P. Yang: Angew. Chem. **42** (2003) 3031. https://doi.org/10.1002/anie.200351461
30 K. H. Baik, J. Kim, and S. Jang: Appl. Surf. Sci. **435** (2018) 592. https://doi.org/10.1016/j.apsusc.2017.11.038
31 K. Wetchakun, T. Samerjal, N. Tamaekong, C. Liewhiran, C. Siriwong, V. Kruefu, A. Wisitsoraat, A. Tuantranont, and S. Phanichphant: Sens. Actuators, B **160** (2011) 580. https://doi.org/10.1016/j.snb.2011.08.032
32 C. Wen, Q. Ye, S. L. Zhang, and D. Wu: Sens. Actuators, B **223** (2016) 791. https://doi.org/10.1016/j.snb.2015.10.019

About the Authors

Kwang Hyeon Baik received his B.S. degree from Yonsei University, Seoul, Korea, in 1998 and his Ph.D. degree in materials science and engineering from University of Florida, Gainesville, Florida, in 2004. He worked at the Photonics Lab at Samsung Advanced Institute of Technology from 2005 to 2008 and also worked at Korea Electronics Technology Institute from 2009 to 2011. Since 2012, he has been with Hongik University, Sejong, Korea as an associate professor. His current research interests include the growth and characterization of GaN- and ZnO-based light-emitting diodes and hydrogen gas sensors, and III–V semiconductor-based electronic devices. (khbaik@hongik.ac.kr)

Soohwan Jang received his B.S. degree from the Department of Chemical Engineering, Seoul National University, Seoul, Korea, in 2003 and his Ph.D. degree from the Department of Chemical Engineering, University of Florida, Gainesville, Florida, in 2007. From 2007 to 2009, he worked at Samsung Electronics. He has been a professor at the Department of Chemical Engineering, Dankook University, since 2009. His research interests include nitride- and oxide-based sensors, light-emitting diodes, and integrated electronic devices.
(jangmountain@dankook.ac.kr)